

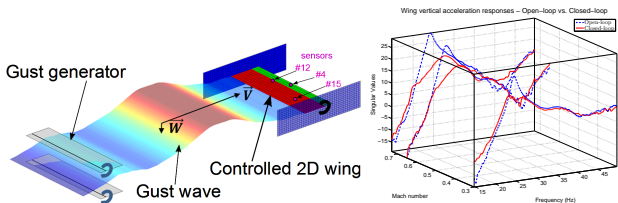
Identification and robust load control in response to gust

... from subsonic to transonic, a wind tunnel application

C. Pousset-Vassal, F. Demourant &
 A. Lepage, D. Le Bihan



April 2015, Onera



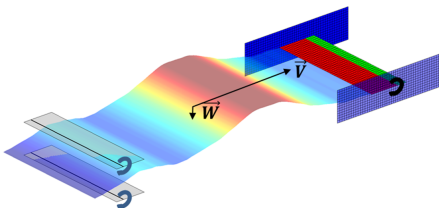
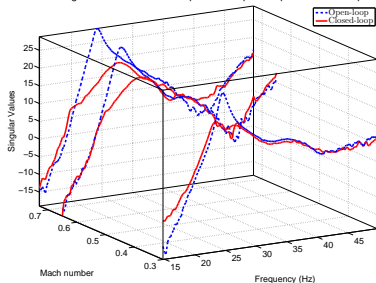
Load and vibration control...

Loads alleviation and vibration reduction is crucial in aeronautics for **structure stress and fatigue reduction, potential wing weight reduction, consumption reduction, lifetime enhancement. . .**

Amount the potential lever:

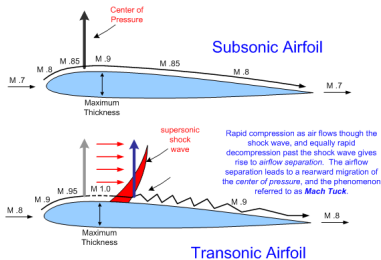
- ▶ Passive solution (aeroelasticity, material, shape, . . .)
- ▶ **Active solutions** (control law, actuators, . . .)

Wing vertical acceleration responses – Open-loop vs. Closed-loop



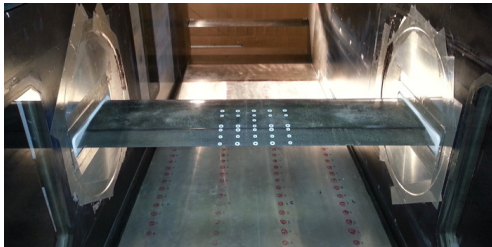
Many challenges are presents:

- ▶ Complex disturbance (discrete, large spectrum ...)
- ▶ Limited actuator and computer burden
- ▶ **System flexibility and aeroelasticity**
- ▶ **Operate over a wide range of flight conditions** (subsonic, transonic)



A control approach...

- ▶ Experimental set-up
- ▶ Dynamical modelling & control design
- ▶ Implementation & results



(video)

Experimental set-up

- Wind tunnel set-up (DAFE & DADS, Meudon, France)

- Controlled aeroelastic wing (DADS)

- Open-loop experiments (DADS & DAFE)

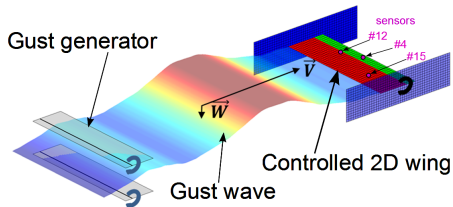
Modelling and identification

Control design

Epilogue

Wind tunnel set-up (DAFE & DADS, Meudon, France)

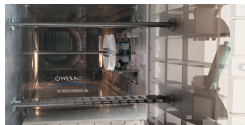
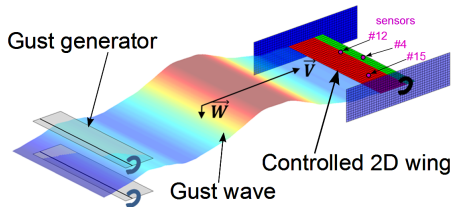
- ▶ Wind Tunnel at Onera S3Ch
- ▶ Gust generator
- ▶ 2D wing profile, many accelerometers and one single control surface
- ▶ **Interest in working in a "controlled" area to master the disturbances**



Experimental set-up

Wind tunnel set-up (DAFE & DADS, Meudon, France)

- ▶ Wind Tunnel at Onera S3Ch
- ▶ Gust generator
- ▶ 2D wing profile, many accelerometers and one single control surface
- ▶ **Interest in working in a "controlled" area to master the disturbances**

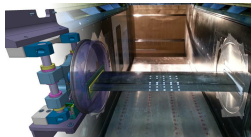
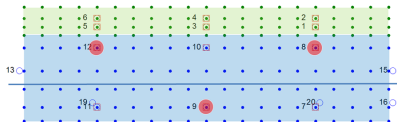


(i) wind tunnel (ii) gust generator (iii) flow stream trajectory and controlled wing

Experimental set-up

Controlled aeroelastic wing (DADS)

- ▶ Dynamics along vertical and rotational axis
- ▶ Additional structure models (torsion, bending, ...)
- ▶ Controlled surface along the wingspan (angle) & angle of attack

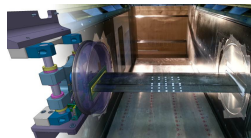
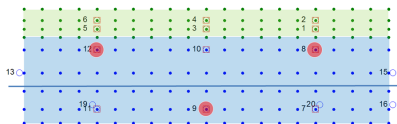


(i) schematic view of the wing (ii) controlled system facing the wind

Experimental set-up

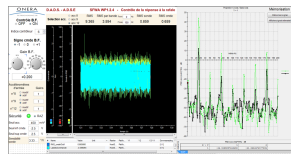
Controlled aeroelastic wing (DADS)

- ▶ Dynamics along vertical and rotational axis
- ▶ Additional structure models (torsion, bending, ...)
- ▶ Controlled surface along the wingspan (angle) & angle of attack



(i) schematic view of the wing (ii) controlled system facing the wind

- ▶ About 20 accelerometers
- ▶ Controlled wind and disturbances
- ▶ Acquisition system

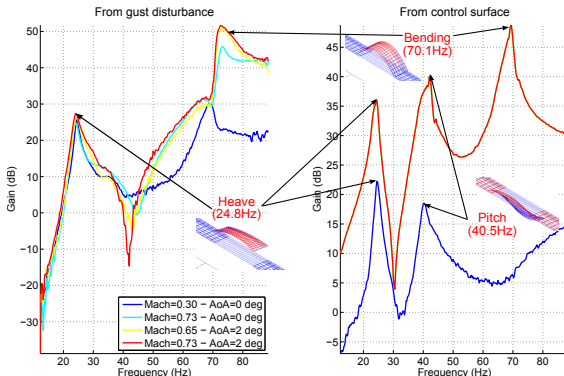


(iii) DADS interface

Experimental set-up

Open-loop experiments (DADS & DAFE)

- ▶ Many weeks of work for calibrating the gust generator
- ▶ Many iterations for obtaining open-loop controlled wing surface transfer
- ▶ Set-up of an acquisition system



(i) some open-loop results...

Experimental set-up

Modelling and identification

- Problem formulation

- First approach: Loewner framework

- Second approach: subspace with LMI constraint

- Some conclusions

Control design

Epilogue

Problem

Given frequency samples ω_i and responses $\Phi_i \in \mathbb{C}^{n_y \times n_u}$

$$H(j\omega_i) = \Phi_i, i = 1, \dots, N. \quad (1)$$

where H is the **exact** transfer function of the system, the objective is to obtain a r th-order rational LTI model of the form, $\hat{H}(s) = \hat{C}(s\hat{E} - \hat{A})^{-1}\hat{B} + \hat{D} \in \mathcal{H}_\infty^{n_y \times n_u}$, with realization defined as:

$$\hat{\mathbf{H}} : \hat{E}\dot{\hat{\mathbf{x}}}(t) = \hat{A}\hat{\mathbf{x}}(t) + \hat{B}\mathbf{u}(t), \mathbf{y}(t) = \hat{C}\hat{\mathbf{x}}(t) + \hat{D}\mathbf{u}(t), \quad (2)$$

that **well matches the obtained frequency sample $\{\omega_i, \Phi_i\}$ and hopefully reproduces the actual transfer H** . Let $\hat{\mathbf{x}}(t) \in \mathbb{R}^r$, $\mathbf{u}(t) \in \mathbb{R}^{n_u}$ and $\mathbf{y}(t) \in \mathbb{R}^{n_y}$ be the states, inputs and outputs vectors, respectively.

- 1 based on the **Loewner framework**,
- 2 based on the **subspace one with LMI constraints**.

First approach: Loewner framework¹

Set

$$\begin{aligned}
 [\omega_1, \omega_2, \dots, \omega_N] &= [\mu_1, \mu_2, \dots, \mu_n] \cup [\lambda_1, \lambda_2, \dots, \lambda_{\bar{n}}] \\
 [\Phi_1, \Phi_2, \dots, \Phi_N] &= [\tilde{v}_1, \tilde{v}_2, \dots, \tilde{v}_n] \cup [\tilde{w}_1, \tilde{w}_2, \dots, \tilde{w}_{\bar{n}}]
 \end{aligned} \tag{3}$$


and define

- ▶ $\mathbf{l}_i \in \mathbb{C}^{1 \times n_y}$ ($i = 1, \dots, n$) and
- ▶ $\mathbf{r}_j \in \mathbb{C}^{n_u \times 1}$ ($j = 1, \dots, \bar{n}$)

the n left and \bar{n} right tangential directions ($n + \bar{n} = N$). Using these tangential directions, one can then compute

- ▶ $\mathbf{v}_i = \mathbf{l}_i \tilde{v}_i \in \mathbb{C}^{1 \times n_u}$ and
- ▶ $\mathbf{w}_j = \tilde{w}_j \mathbf{r}_j \in \mathbb{C}^{n_y \times 1}$

the left and right tangential values, respectively.

¹  L. Meier III and D. G. Luenberger, "Approximation of linear constant systems", IEEE Transactions on Automatic Control, vol. 12, no. 5, pp. 585-588, 1967.

First approach: Loewner framework - Exact interpolation²

General interpolation problem

Given *left* and *right interpolation data*:

$$\{(\mu_i, \mathbf{l}_i, \mathbf{v}_i) | \mu_i \in \mathbb{C}, \mathbf{l}_i \in \mathbb{C}^{1 \times n_y}, \mathbf{v}_i \in \mathbb{C}^{1 \times n_u}, i = 1, \dots, \underline{n}\} \quad (4)$$

$$\{(\lambda_j, \mathbf{r}_j, \mathbf{w}_j) | \lambda_j \in \mathbb{C}, \mathbf{r}_j \in \mathbb{C}^{n_u \times 1}, \mathbf{w}_j \in \mathbb{C}^{n_y \times 1}, j = 1, \dots, \bar{n}\} \quad (5)$$

construct a realization $\mathbf{H} = (E, A, B, C, 0)$ of appropriate dimensions whose transfer function $H(s) = C(sE - A)^{-1}B$ both satisfies the *left* and *right constraints*:

$$\mathbf{l}_i H(\mu_i) = \mathbf{v}_i, \quad i = 1, \dots, \underline{n} \quad (6)$$

$$H(\lambda_j) \mathbf{r}_j = \mathbf{w}_j, \quad j = 1, \dots, \bar{n}. \quad (7)$$

² 

L. Meier III and D. G. Luenberger, "Approximation of linear constant systems", IEEE Transactions on Automatic Control, vol. 12, no. 5, pp. 585-588, 1967.

Theorem: Loewner interpolation

Given *left* and *right interpolation data* as in (4)-(5), and assuming that $\underline{n} = \bar{n} = \check{n}$, the \check{n} -th order rational transfer function $H(s) = C(sE - A)^{-1}B$, with realization $\mathbf{H} = (E, A, B, C, 0)$ constructed as

$$E = -\mathbb{L}, \quad A = -\mathbb{L}_\sigma, \quad B = V \quad \text{and} \quad C = W, \quad (8)$$

interpolates the left and right constraints (6)-(7), if

$$\begin{aligned} [\mathbb{L}]_{ij} &= \frac{\mathbf{v}_i \mathbf{r}_j - \mathbf{l}_i \mathbf{w}_j}{\mu_i - \lambda_j} = \frac{\mathbf{l}_i (H(\lambda_i) - H(\mu_j)) \mathbf{r}_j}{\mu_i - \lambda_j} \\ [\mathbb{L}_\sigma]_{ij} &= \frac{\mu_i \mathbf{v}_i \mathbf{r}_j - \mathbf{l}_i \mathbf{w}_j \lambda_j}{\mu_i - \lambda_j} = \frac{\mu_i \mathbf{l}_i (H(\lambda_i) - H(\mu_j)) \mathbf{r}_j \lambda_j}{\mu_i - \lambda_j} \end{aligned} \quad (9)$$

known as the Loewner and the shifted Loewner matrices, respectively, and $W = [\mathbf{w}_1, \dots, \mathbf{w}_{\check{n}}]$, $V^T = [\mathbf{v}_1^T, \dots, \mathbf{v}_{\check{n}}^T]$.

³ 

A. Ionita and A. Antoulas, "Data-driven parametrized model reduction in the Loewner framework", SIAM Journal on Scientific Computing, vol. 36, no. 3, pp. 984-1007, 2014.

Theorem: Loewner approximation

To obtain a reduced order model $\hat{\mathbf{H}}$ of order $r \leq n$ that well approximates \mathbf{H} one should simply apply a **SVD** as follows:

$$\mathbf{L} = \begin{bmatrix} Y_1 & Y_2 \end{bmatrix} \begin{bmatrix} \Sigma_1 & \\ & \Sigma_2 \end{bmatrix} \begin{bmatrix} X_1^* \\ X_2^* \end{bmatrix} \quad (10)$$

where $\Sigma_1 \in \mathbb{R}^{r \times r}$, $\Sigma_2 \in \mathbb{R}^{(n-r) \times (n-r)}$ and Y_1, Y_2, X_1, X_2 of appropriate dimensions. Then the reduced order model is simply obtained by the Petrov-Galerkin projection:

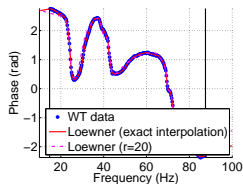
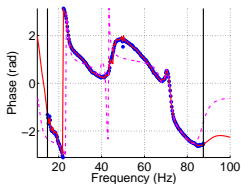
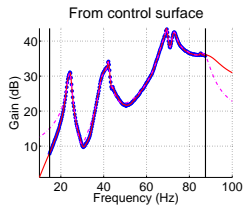
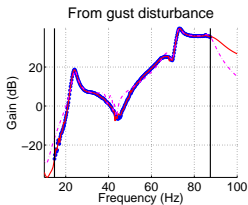
$$\begin{aligned} \hat{\mathbf{H}} &= (\hat{E}, \hat{A}, \hat{B}, \hat{C}, 0) \\ &= (-Y_1^* \mathbf{L} X_1, -Y_1^* \mathbf{L}_\sigma X_1, Y_1^* V, C X_1, 0). \end{aligned} \quad (11)$$

⁴  A. Ionita and A. Antoulas, "Data-driven parametrized model reduction in the Loewner framework", SIAM Journal on Scientific Computing, vol. 36, no. 3, pp. 984-1007, 2014.

Modelling and identification

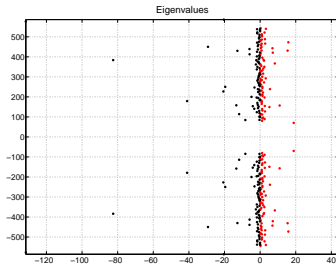
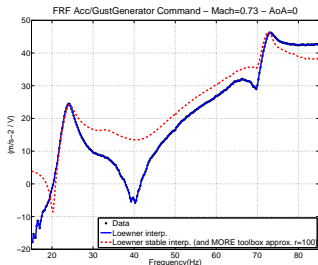
First approach: Loewner framework - MORE toolbox (Mach 0.70, AoA 0deg)

- ▶ $N = 584$ sampled data points, $n_y = 3$ outputs and $n_u = 2$ inputs,
- ▶ $\underline{n} = \bar{n} = \check{n} = 292$, and $r = 20$.



Modelling and identification

First approach: Loewner framework - Some issues

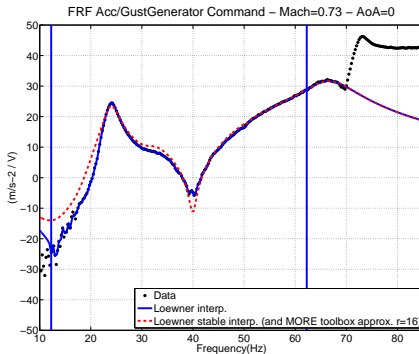


(i) illustration of a problem (ii) Eigenvalues of the Loewner approximation

→ However, some issues have to be handled:

- ▶ interpolant of high dimension,
- ▶ and unstable,
- ▶ selection of tangential directions.

First approach: Loewner framework - Some issues



(i) a clue to handle \mathcal{H}_2 optimality objective and the l_2 one

- ▶ discrete filtering
- ▶ sampling
- ▶ ...?

Define a framework in the discrete-domain:

- ▶ Let us first consider the frequency domain discrete state-space representation:

$$\begin{aligned} e^{z\omega} X(\omega) &= AX(\omega) + BU(\omega) \\ Y(\omega) &= CX(\omega) + DU(\omega) \end{aligned} \quad (12)$$

- ▶ Moreover, if a discrete frequency domain data set $\{\omega_i, \Phi_i\}$ ($i = 1, \dots, N$) is considered then, one has $G(\omega_i) = \Phi_i$ and the following relation holds:

$$\mathbf{G} = O\mathbf{X}^c + \Gamma\mathbf{W} \quad (13)$$

$$\mathbf{G} = \begin{bmatrix} \Phi_1 & \dots & \Phi_N \\ e^{z\omega_1} \Phi_1 & \dots & e^{z\omega_N} \Phi_N \\ \vdots & \ddots & \vdots \\ e^{z(q-1)\omega_1} \Phi_1 & \dots & e^{z(q-1)\omega_N} \Phi_N \end{bmatrix} \in \mathbb{C}^{n_y q \times n_u N}$$

Modelling and identification

Second approach: subspace with LMI constraint

$$\mathbf{G} = \mathbf{O}\mathbf{X}^c + \mathbf{\Gamma}\mathbf{W} \quad (14)$$

$$\mathbf{X}^c = [X^c(i\omega_1), \dots, X^c(i\omega_N)] \in \mathbb{C}^{n \times n_u N}, \quad \mathbf{O} = \begin{bmatrix} C \\ CA \\ \vdots \\ CA^{q-1} \end{bmatrix} \in \mathbb{R}^{n_y q \times n}$$

and

$$\mathbf{W} = \begin{bmatrix} I_{n_u} & \dots & I_{n_u} \\ e^{i\omega_1} I_{n_u} & \dots & e^{i\omega_N} I_{n_u} \\ \vdots & \ddots & \vdots \\ e^{i(q-1)\omega_1} I_{n_u} & \dots & e^{i(q-1)\omega_N} I_{n_u} \end{bmatrix} \in \mathbb{C}^{n_u q \times n_u N}$$

$$\mathbf{\Gamma} = \begin{bmatrix} D & 0 & \dots & 0 \\ CB & D & \dots & 0 \\ \vdots & \vdots & \ddots & \vdots \\ CA^{q-2}B & CA^{q-3}B & \dots & D \end{bmatrix} \in \mathbb{R}^{n_y q \times n_u q}.$$

Second approach: subspace with LMI constraint

- ▶ The extended observability matrix O , which depends on A and C , can be written as a combination of inputs/outputs data \mathbf{G} , \mathbf{X}^c , and \mathbf{W} , only. Then, an elegant way to extract A and C matrices from O , is to first apply an orthogonal projection \mathbf{W}^\perp defined as

$$\mathbf{W}^\perp = I - \mathbf{W}^T(\mathbf{W}\mathbf{W}^T)^{-1}\mathbf{W}, \quad (15)$$

- ▶ Indeed, by right multiplying with \mathbf{W}^\perp , the following is obtained:

$$\mathbf{G}\mathbf{W}^\perp = O\mathbf{X}^c\mathbf{W}^\perp.$$

- ▶ Then, an effective way to extract A and C is to use a **QR** and a **SVD** of $\mathbf{G}\mathbf{W}^\perp$, and by noticing that

$$\begin{aligned} \mathbf{G}\mathbf{W}^\perp = R_{22}Q_2^T &= \hat{U}\hat{\Sigma}\hat{V}^T Q_2^T \\ &= [\hat{U}_s \quad \hat{U}_0] \begin{bmatrix} \hat{\Sigma}_s & 0 \\ 0 & \hat{\Sigma}_o \end{bmatrix} \begin{bmatrix} \hat{V}_s^T \\ \hat{V}_o^T \end{bmatrix} Q_2^T. \end{aligned}$$

Second approach: subspace with LMI constraint

- ▶ \hat{A} and \hat{C} are obtained as

$$\hat{A} = (J_1 \hat{U}_s)^\dagger J_2 \hat{U}_s$$

$$\hat{C} = J_3 \hat{U}_s$$

where

$$J_1 = \begin{bmatrix} I_{(q-1)n_y} & 0_{(q-1)n_y \times n_y} \end{bmatrix}$$

$$J_2 = \begin{bmatrix} 0_{(q-1)n_y \times n_y} & I_{(q-1)n_y} \end{bmatrix}$$

$$J_3 = \begin{bmatrix} I_{n_y} & 0_{n_y \times (q-1)n_y} \end{bmatrix}$$

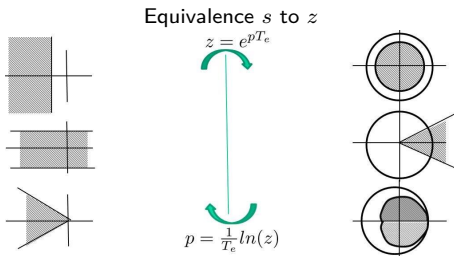
- ▶ \hat{B} and \hat{D} are obtained as

$$\{\hat{B}, \hat{D}\} = \arg \min_{\substack{\hat{B} \in \mathbb{R}^{n \times n_u} \\ \hat{D} \in \mathbb{R}^{n_y \times n_u}}} \sum_{k=1}^N \|\Phi_{\mathbf{k}} - \hat{H}(\omega_{\mathbf{k}}, \hat{B}, \hat{D})\|_F^2.$$

Modelling and identification

Second approach: subspace with LMI constraint - LMI regions

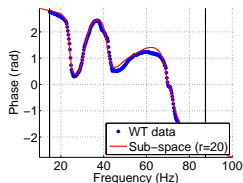
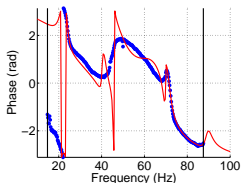
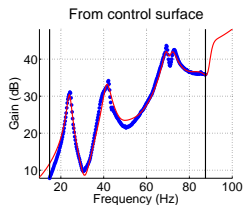
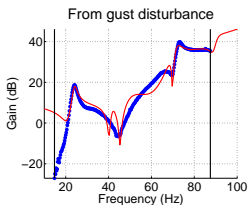
$\mathbf{Re}(z) < 0$	\Leftrightarrow	$z + \bar{z} < 0$	\Leftrightarrow	left side
$\mathbf{Re}(z) < -\alpha$	\Leftrightarrow	$z + \bar{z} + 2\alpha < 0$	\Leftrightarrow	shifted left side
$ z < r$	\Leftrightarrow	$\begin{pmatrix} -r & z \\ \bar{z} & -r \end{pmatrix} < 0$	\Leftrightarrow	disc with radius lower than r
$\alpha_1 < \mathbf{Re}(z) < \alpha_2$	\Leftrightarrow	$\begin{pmatrix} z + \bar{z} - 2\alpha_2 & 0 \\ 0 & z + \bar{z} + 2\alpha_1 \end{pmatrix} < 0$	\Leftrightarrow	vertical strips
$\mathbf{Re}(z)\tan(\theta) < - \mathbf{Im}(z) $	\Leftrightarrow	$\begin{pmatrix} (z + \bar{z})\sin\theta & (z - \bar{z})\cos\theta \\ (z - \bar{z})\cos\theta & (z + \bar{z})\sin\theta \end{pmatrix} < 0$	\Leftrightarrow	conic region



Modelling and identification

Second approach: subspace with LMI constraint - MORE toolbox (Mach 0.70, AoA 0deg)

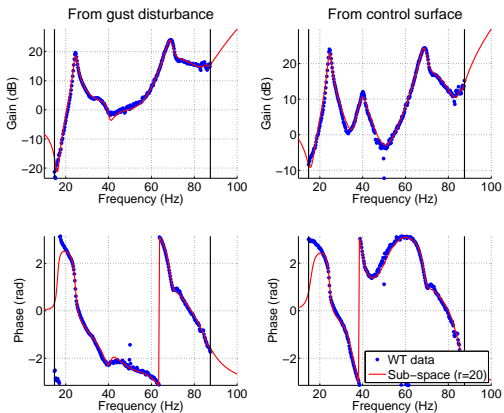
- ▶ $N = 584$ sampled data points, $n_y = 3$ outputs and $n_u = 2$ inputs,
- ▶ LMI region and $r = 20$.



Modelling and identification

Second approach: subspace with LMI constraint - MORE toolbox (Mach 0.70, AoA 0deg)

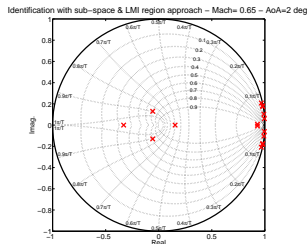
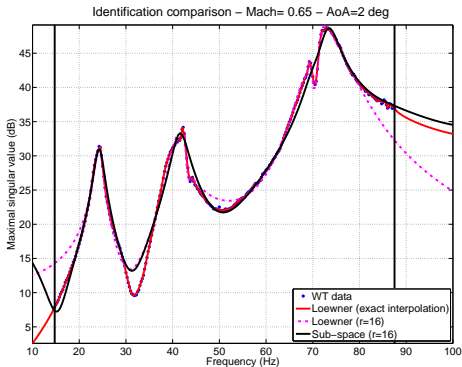
- ▶ $N = 292$ sampled data points, $n_y = 3$ outputs and $n_u = 2$ inputs,
- ▶ LMI region and $r = 20$.



Modelling and identification

Some conclusions

- ▶ Two nice approaches
- ▶ However, the Loewner approach cannot guarantee pole location



Experimental set-up

Modelling and identification

Control design

Structured LTI robust controller

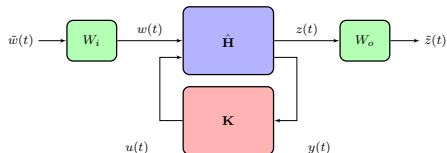
Real-time implementation (user-friendly interface)

Results


Epilogue

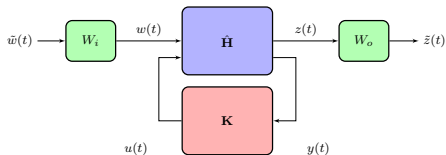
Structured LTI robust controller⁵

$$K^* := \underset{\substack{\text{rank}(K) = n_c \\ K \in \mathcal{K} \subseteq \mathcal{H}_2^{1 \times 2}}}{\text{argmin}} \left\| \begin{bmatrix} T_{\bar{w} \rightarrow \bar{z}}^{(1)}(K) \\ \vdots \\ T_{\bar{w} \rightarrow \bar{z}}^{(n_s)}(K) \end{bmatrix} \right\|_{\mathcal{H}_\infty} \quad (17)$$



- ▶ \mathcal{K} is the set of all stable rational functions with derivative action and roll-off of second order
- ▶ $T_{\bar{w} \rightarrow \bar{z}}^{(i)}(G) = W_i \mathcal{F}_l(\hat{H}^{(i)}, G) W_o$, as described on the above figure ($i = 1, \dots, n_s$)

⁵  P. Apkarian and D. Noll, "Nonsmooth \mathcal{H}_∞ Synthesis", in IEEE Transaction in Automatic Control, Vol. 51(1), January, 2006, pp. 71-86.


Structured LTI robust controller⁶

$$W_o(s) = \begin{bmatrix} W_p(s) & 0 \\ 0 & W_u(s) \end{bmatrix} \text{ and } W_i(s) = 1 \quad (18)$$

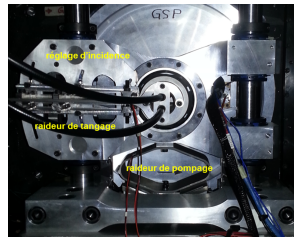
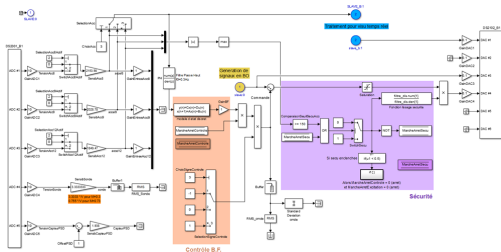
$$W_p(s) = \frac{G(s/10w_p + 1)}{s/w_p + 1} I_2 \quad (19)$$

$$W_u(s) = \frac{s/w_{act} + 1}{s/10w_{act} + 1}$$

where G is the \mathcal{H}_∞ -norm of the performance transfer, $w_p = w_{act} = 30 \times 2\pi \text{rad/s}$.

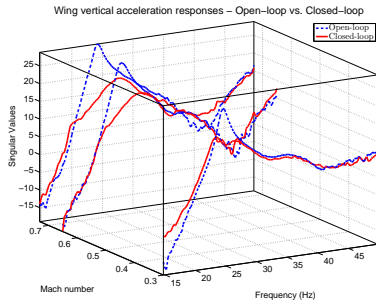
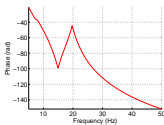
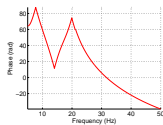
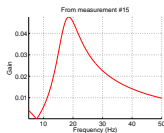
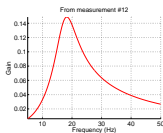
⁶  P. Apkarian and D. Noll, "Nonsmooth \mathcal{H}_∞ Synthesis", in IEEE Transaction in Automatic Control, Vol. 51(1), January, 2006, pp. 71-86.

Real-time implementation (user-friendly interface)



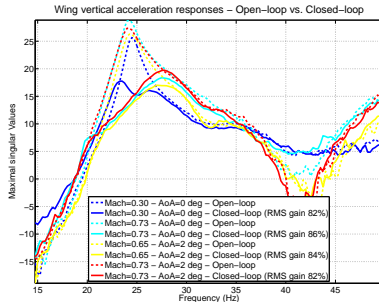
- ▶ Easy to adjust the control law,
- ▶ and after some iterations...

Results - Angle of Attack 0 deg / Mach 0.30 and 0.73



- ▶ Controller structure high pass and roll-off
- ▶ Gain around 10dB at the peak value
- ▶ Robust to Mach variations

Results - Angle of attack 2 deg / Mach 0.65 and 0.73



- ▶ Gain around 10dB at the peak value
- ▶ Robust to Mach variations & AoA

Experimental set-up

Modelling and identification

Control design

Epilogue

What to keep in mind?

... and next steps

What to keep in mind?

- ▶ WTT performed at Onera S3Ch
- ▶ **2 frequency-domain identification procedures** (numerically robust)
- ▶ **Robust active control solution** implemented on a real-time computer
- ▶ Attenuation at **sub and transonic conditions: first time in Europe**



... and next steps

Forthcoming challenges

Bench Move toward 3D wing profile & more flexible wings [Clean Sky 2]

Publi Publish results [IEEE trans. CST]


Methods Enhanced modelling procedures [Data-based \mathcal{H}_2 model approximation]^{a b c}


Methods Parametric / adaptive control

Mixed Use additional and/or different actuators (e.g. pulsed fluid)



^a  Z. Drmac, S. Gugercin and C.A. Beattie, "*Vector Fitting for Matrix-valued Rational Approximation*", Submitted. Available as arXiv:1503.00411.

^b  I. Pontes Duff Pereira, C. Pousot-Vassal and C. Seren, "*Realization independent single time-delay dynamical model interpolation and H2-optimal approximation*", submitted.

^c  C. Pousot-Vassal and P. Vuillemin, "*Introduction to MORE: a MOdel REDuction Toolbox*", In Proceedings of the IEEE Multi-conference on Systems and Control (MSC CCA'12), Dubrovnik, Croatia, October, 2012, pp. 776-781.

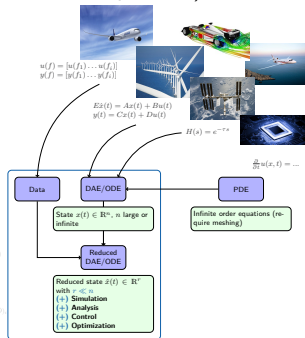
(Some) Acknowledgements

- DADS Arnaud Lepage (project leader),
- DADS Dominique Le Bihan (modelling and control),
- DADS Yannick Amosse (mechanical integration),
- DAFE Jean-Charles Abart (S3Ch Meudon wind tunnel responsible),
- DAFE Vincent Brion (wind tunnel engineer)



MORE toolbox

► <http://w3.onera.fr/more/>



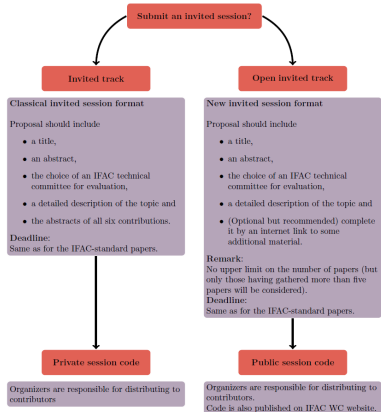
Announcement

Forthcomming 20th IFAC WC, Toulouse, France (2017)

New invited session format

- ▶ classical invited sessions or
- ▶ new open invited tracks

More on <https://www.ifac2017.org/invited>



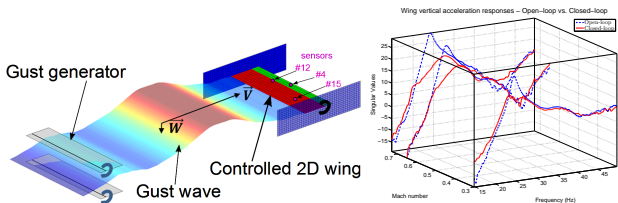
Identification and robust load control in response to gust

... from subsonic to transonic, a wind tunnel application

C. Pousset-Vassal, F. Demourant &
A. Lepage, D. Le Bihan



April 2015, Onera



Proof of the subspace approach with LMI constraints

... and next steps

$J_1 \hat{U}_s \hat{A} = J_2 \hat{U}_s \Leftrightarrow \hat{A} = (J_1 \hat{U}_s)^\dagger J_2 \hat{U}_s \Leftrightarrow \hat{A} = \varphi^\dagger b$ avec $\varphi = J_1 \hat{U}_s$ et $b = J_2 \hat{U}_s$. Or
 $\hat{A} = \varphi^\dagger b \Leftrightarrow \hat{A} \Psi = \varphi^\dagger b \Psi \Leftrightarrow \tilde{A} = \varphi^\dagger b \Psi \Leftrightarrow \min \|\varphi \tilde{A} - b \Psi\|_2^2$

Moreover

$$\min \|\varphi \tilde{A} - b \Psi\|_2^2 \Leftrightarrow \min_{\beta \in \mathbf{R}} \beta > 0 \quad (\varphi \tilde{A} - b \Psi)^T (\varphi \tilde{A} - b \Psi) < \beta$$

From Schur lemma:

$$\begin{aligned} & (\varphi \tilde{A} - b \Psi)^T (\varphi \tilde{A} - b \Psi) < \beta \\ \Leftrightarrow & (\varphi \tilde{A} - b \Psi)^T (\varphi \tilde{A} - b \Psi) - \beta < 0 \\ \Leftrightarrow & \begin{pmatrix} I & (\varphi \tilde{A} - b \Psi) \\ (\varphi \tilde{A} - b \Psi)^T & \beta \end{pmatrix} > 0 \end{aligned}$$

From Chilali and Gahinet proposition:

$P \otimes \Psi + Q \otimes \tilde{A} \Psi + Q^T \otimes (\tilde{A} \Psi)^T < 0 \Leftrightarrow P \otimes \Psi + Q \otimes \tilde{A} + Q^T \otimes \tilde{A}^T < 0$
 where $\tilde{A} = \hat{A} \Psi$ et $\Psi = \Psi^T > 0$